Contents lists available at ScienceDirect

J. Math. Anal. Appl.

www.elsevier.com/locate/jmaa

A type of bounded traveling wave solutions for the Fornberg–Whitham equation

Jiangbo Zhou *, Lixin Tian

Nonlinear Scientific Research Center, Faculty of Science, Jiangsu University, Zhenjiang, Jiangsu 212013, China

ARTICLE INFO

ABSTRACT

In this paper, by using bifurcation method, we successfully find the Fornberg–Whitham equation

$$u_t - u_{xxt} + u_x = uu_{xxx} - uu_x + 3u_x u_{xx},$$

has a type of traveling wave solutions called kink-like wave solutions and antikink-like wave solutions. They are defined on some semifinal bounded domains and possess properties of kink waves and anti-kink waves. Their implicit expressions are obtained. For some concrete data, the graphs of the implicit functions are displayed, and the numerical simulation is made. The results show that our theoretical analysis agrees with the numerical simulation.

Crown Copyright © 2008 Published by Elsevier Inc. All rights reserved.

1. Introduction

It is well known that the exact solutions for the nonlinear partial differential equations can help people know deeply the described process. So an important issue of the nonlinear partial differential equations is to find their new exact solutions. Traveling wave solution is an important type of solution for the nonlinear partial differential equations and many nonlinear partial differential equations have been found to have a variety of traveling wave solutions. For instances, the well-known Korteweg–de Vries equation

$$u_t - 6uu_x + uu_{xxx} = 0 \tag{1.1}$$

has solitary wave solutions and its solitary waves are solitons [1]. A KdV-like equation

$$u_t + a(1 + bu^n)u^n u_x + \delta u_{xxx} = 0 \tag{1.2}$$

has some kink wave solutions [2]. Its kink wave solution $u(\xi)$ $(\xi = x - ct)$ was defined on $(-\infty, +\infty)$, and $\lim_{\xi \to -\infty} u(\xi) = A$, $\lim_{\xi \to \infty} u(\xi) = B$, where A and B are two constants and $A \neq B$. The Camassa–Holm equation

$$u_t - u_{xxt} + 3uu_x = 2u_x u_{xx} + uu_{xxx} \tag{1.3}$$

has peakons, cuspons, stumpons, composite wave solutions [3]. It also has compactons [4]. The Degasperis–Procesi equation

$$u_t - u_{xxt} + 4uu_x = 3u_x u_{xx} + uu_{xxx} \tag{1.4}$$

---

* Corresponding author.
  E-mail addresses: zhoujiangbo@yahoo.cn (J. Zhou), tianlx@ujs.edu.cn (L. Tian).

has a multitude of peculiar wave solutions: peakons, cuspons, composite waves, and stumpons [5]. The Kuramoto–Sivashinsky equation

$$u_t + uu_x + u_{xx} + u_{xxxx} = 0 \tag{1.5}$$

has periodic and solitary solutions [6]. In [7], Liu, Li and Lin found a new type of traveling wave solutions for the Camassa–Holm equation, which are defined on some semifinal bounded domains and possess properties of kink waves or anti-kink waves. They called them kink-like waves and antikink-like waves. Later, Guo and Liu [8] found the CH-γ equation

$$u_t + c_0 u_x + 3uu_x - \alpha^2(u_{xxt} + uu_{xxx} + 3u_x u_{xx}) + \gamma u_{xxx} = 0, \tag{1.6}$$

posses kink-like waves when $\alpha^2 > 0$. Tang and Zhang [9] showed the CH-γ equation (1.6) also has kink-like wave solutions even when $\alpha^2 < 0$. Chen and Tang [10] showed that the Degasperis–Procesi equation (1.4) has such type of traveling wave solutions. Recently, Liu and Yao [11] found the following generalized Camassa–Holm equation:

$$u_t + 2ku_x - u_{xxt} + auu_x = 2u_x u_{xx} + uu_{xxx} \tag{1.7}$$

also posses kink-like wave solutions.

We are motivated to seek kink-like wave and antikink-like wave solutions for the Fornberg–Whitham equation

$$u_t - u_{xxt} + u_x = uu_{xxx} - uu_x + 3u_x u_{xx}. \tag{1.8}$$

To our knowledge, such type of traveling wave solution has never been found for the Fornberg–Whitham equation. Eq. (1.8) was used to study the qualitative behaviors of wave-breaking [12]. It admits a wave of greatest height, as a peaked limiting form of the traveling wave solution [13], $u(x,t) = A \exp(\frac{1}{2}|x - \frac{4}{3}t|)$, where A is an arbitrary constant.

The remainder of the paper is organized as follows. In Section 2, we state the main results which are implicit expressions of the kink-like wave and the antikink-like wave solutions. In Section 3, we give the proof of the main results. In Section 4, we make the numerical simulation of the kink-like and the antikink-like waves. A short conclusion is given in Section 5.

2. Main results

We state our main result as follows.

Theorem 1. *For given constant c, let*

$$\xi = x - ct, \tag{2.1}$$

$$\varphi_0^\pm = c - 1 \pm \sqrt{(c-1)^2 - 2g}, \tag{2.2}$$

$$g_1(c) = \frac{(c-1)^2}{2}, \tag{2.3}$$

$$g_2(c) = \frac{(c-1)^2 - 1}{2}. \tag{2.4}$$

(1) *If $g < g_2(c)$, then Eq. (1.8) has two kink-like wave solutions $u = \varphi_1(\xi)$ and $u = \varphi_3(\xi)$ and two antikink-like wave solutions $u = \varphi_2(\xi)$ and $u = \varphi_4(\xi)$.*

$$\frac{(2\sqrt{\varphi_1^2 + l_1\varphi_1 + l_2} + 2\varphi_1 + l_1)(\varphi_1 - \varphi_0^-)^{\alpha_1}}{(2\sqrt{a_1}\sqrt{\varphi_1^2 + l_1\varphi_1 + l_2} + b_1\varphi_1 + l_3)^{\alpha_1}} = \beta_1 e^{-\frac{1}{2}\xi}, \quad \xi \in \left(-\infty, \xi_0^1\right), \tag{2.5}$$

$$\frac{(2\sqrt{\varphi_2^2 + l_1\varphi_2 + l_2} + 2\varphi_2 + l_1)(\varphi_2 - \varphi_0^-)^{\alpha_1}}{(2\sqrt{a_1}\sqrt{\varphi_2^2 + l_1\varphi_2 + l_2} + b_1\varphi_2 + l_3)^{\alpha_1}} = \beta_1 e^{\frac{1}{2}\xi}, \quad \xi \in \left(-\xi_0^1, \infty\right), \tag{2.6}$$

$$\frac{(2\sqrt{\varphi_3^2 + m_1\varphi_3 + m_2} + 2\varphi_3 + m_1)(\varphi_3 - \varphi_0^+)^{\alpha_2}}{(2\sqrt{a_2}\sqrt{\varphi_3^2 + m_1\varphi_3 + m_2} + b_2\varphi_2 + m_3)^{\alpha_2}} = \beta_2 e^{-\frac{1}{2}\xi}, \quad \xi \in \left(-\xi_0^3, \infty\right), \tag{2.7}$$

and

$$\frac{(2\sqrt{\varphi_4^2 + m_1\varphi_4 + m_2} + 2\varphi_4 + m_1)(\varphi_4 - \varphi_0^+)^{\alpha_2}}{(2\sqrt{a_2}\sqrt{\varphi_4^2 + m_1\varphi_4 + m_2} + b_2\varphi_4 + m_3)^{\alpha_2}} = \beta_2 e^{\frac{1}{2}\xi}, \quad \xi \in \left(-\infty, \xi_0^3\right), \tag{2.8}$$

where

$$l_1 = \frac{2}{3}\big(1 - 3c - 3\sqrt{(c-1)^2 - 2g}\,\big), \tag{2.9}$$

$$l_2 = \frac{2}{3}\big[1 - 4c + 3c^2 - 3g + (3c+1)\sqrt{(c-1)^2 - 2g}\,\big], \tag{2.10}$$

$$l_3 = \frac{4}{3}\big[2 - 5c + 3c^2 - 6g + (3c+2)\sqrt{(c-1)^2 - 2g}\,\big], \tag{2.11}$$

$$m_1 = \frac{2}{3}\big(1 - 3c + 3\sqrt{(c-1)^2 - 2g}\,\big), \tag{2.12}$$

$$m_2 = \frac{2}{3}\big[1 - 4c + 3c^2 - 3g - (3c+1)\sqrt{(c-1)^2 - 2g}\,\big], \tag{2.13}$$

$$m_3 = \frac{4}{3}\big[2 - 5c + 3c^2 - 6g - (3c+2)\sqrt{(c-1)^2 - 2g}\,\big], \tag{2.14}$$

$$a_1 = 4\big(1 - 2c + c^2 - 2g + \sqrt{(c-1)^2 - 2g}\,\big), \tag{2.15}$$

$$a_2 = 4\big(1 - 2c + c^2 - 2g - \sqrt{(c-1)^2 - 2g}\,\big), \tag{2.16}$$

$$b_1 = -\frac{4}{3} - 4\sqrt{(c-1)^2 - 2g}, \tag{2.17}$$

$$b_2 = -\frac{4}{3} + 4\sqrt{(c-1)^2 - 2g}, \tag{2.18}$$

$$\alpha_1 = -\frac{1 + \sqrt{(c-1)^2 - 2g}}{2\sqrt{(c-1)^2 - 2g + \sqrt{(c-1)^2 - 2g}}}, \tag{2.19}$$

$$\alpha_2 = \frac{-1 + \sqrt{(c-1)^2 - 2g}}{2\sqrt{(c-1)^2 - 2g - \sqrt{(c-1)^2 - 2g}}}, \tag{2.20}$$

$$\beta_1^0 = \frac{(2\sqrt{c^2 + l_1 c + l_2} + 2c + l_1)(c - \varphi_0^-)^{\alpha_1}}{(2\sqrt{a_1}\sqrt{c^2 + l_1 c + l_2} + b_1 c + l_3)^{\alpha_1}}, \tag{2.21}$$

$$\beta_2^0 = \frac{(2\sqrt{c^2 + m_1 c + m_2} + 2c + m_1)(c - \varphi_0^+)^{\alpha_2}}{(2\sqrt{a_2}\sqrt{c^2 + m_1 c + m_2} + b_2 c + m_3)^{\alpha_2}}, \tag{2.22}$$

$$\beta_1 = \ln\frac{(2\sqrt{a^2 + l_1 a + l_2} + 2a + l_1)(a - \varphi_0^-)^{\alpha_1}}{(2\sqrt{a_1}\sqrt{a^2 + l_1 a + l_2} + b_1 a + l_3)^{\alpha_1}}, \tag{2.23}$$

$$\beta_2 = \frac{(2\sqrt{b^2 + m_1 b + m_2} + 2b + m_1)(b - \varphi_0^+)^{\alpha_2}}{(2\sqrt{a_2}\sqrt{b^2 + m_1 b + m_2} + b_2 b + m_3)^{\alpha_2}}, \tag{2.24}$$

$$\xi_0^1 = \ln\big(\beta_1 / \beta_1^0\big), \tag{2.25}$$

$$\xi_0^3 = \ln\big(\beta_2^0 / \beta_2\big). \tag{2.26}$$

a and b are two constants satisfying $\varphi_1(0) = \varphi_2(0) = a$, $\varphi_3(0) = \varphi_4(0) = b$, and $\varphi_0^- < a < c < b < \varphi_0^+$.

(2) If $g_2(c) \leqslant g \leqslant g_1(c)$, then Eq. (1.8) has a kink-like wave solution $u = \varphi_1(\xi)$ of implicit form (2.5) and an antikink-like wave solution $u = \varphi_2(\xi)$ of implicit form (2.6).

We will give the proof of this theorem in Section 3. Now we take a set of data and employ Maple to display the graphs of $u = \varphi_i(\xi)$ $(i = 1, 2, 3, 4)$.

Example 1. Taking $c = 1$ and $g = -4 < g_2(c)$ (corresponding to (1) of Theorem 1), it follows that $\varphi_0^- = -2.82843$, $\varphi_0^+ = 2.82843$, $l_1 = -6.99019$, $l_2 = 15.5425$, $l_3 = 50.8562$, $a_1 = 43.3137$, $b_1 = -12.647$, $\alpha_1 = -0.581712$. Further, choosing $a = -1 \in (\varphi_0^-, c)$, we obtain $\xi_0^1 = 0.387475$. We present the graphs of the solutions $\varphi_1(\xi)$ and $\varphi_2(\xi)$ in Fig. 1(a) and (b), respectively. Meanwhile, we get $m_1 = 4.32352$ and $m_2 = 0.457528$, $m_3 = 13.1438$, $a_2 = 20.6863$, $b_2 = 9.98038$, $\alpha_2 = 0.40201$. Further, choosing $b = 2 \in (c, \varphi_0^+)$, we get $\xi_0^3 = 0.274787$. The graphs of the solutions $\varphi_3(\xi)$ and $\varphi_4(\xi)$ are presented in Fig. 1(c) and (d), respectively. The graphs in Fig. 1 show that $\varphi_1(\xi)$ and $\varphi_3(\xi)$ are kink-like waves and $\varphi_2(\xi)$ and $\varphi_4(\xi)$ are antikink-like waves.
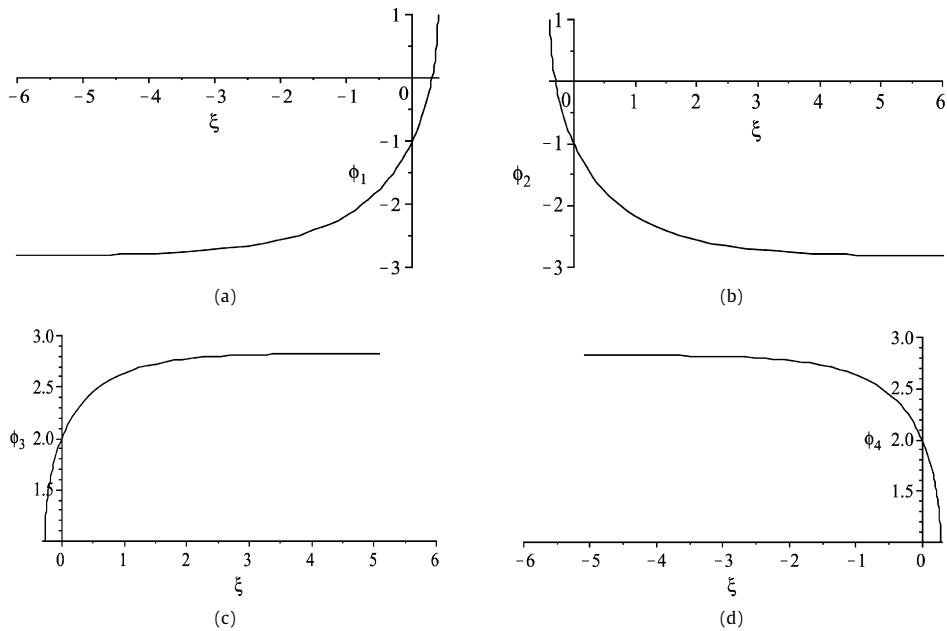
Fig. 1. The graphs of $\varphi_i(\xi)$ ($i = 1, 2, 3, 4$) when $c = 1$, $g = -4$, $a = -1$, $b = 2$.

3. Proof of main results

Let $u = \varphi(\xi)$ with $\xi = x - ct$ be the solution for Eq. (1.8), then it follows that

$$-c\varphi + c\varphi''' + \varphi' = \varphi\varphi''' - \varphi\varphi' + 3\varphi'\varphi''. \tag{3.1}$$

Integrating (3.1) once we have

$$\varphi''(\varphi - c) = g - c\varphi + \varphi + \frac{1}{2}\varphi^2 - (\varphi')^2, \tag{3.2}$$

where g is the integral constant.

Let $y = \varphi'$, then we get the following planar system:

$$\begin{cases} \dfrac{d\varphi}{d\xi} = y, \\ \dfrac{dy}{d\xi} = \dfrac{g - c\varphi + \varphi + \frac{1}{2}\varphi^2 - y^2}{\varphi - c}, \end{cases} \tag{3.3}$$

with a first integral

$$H(\varphi, y) = (\varphi - c)^2 \left[y^2 - \frac{(\varphi - c)^2}{4} - \frac{2}{3}(\varphi - c) - g - c + \frac{c^2}{2} \right] = h, \tag{3.4}$$

where h is a constant.

Note that (3.3) has a singular line $\varphi = c$. To avoid the line temporarily we make transformation $d\xi = (\varphi - c)d\zeta$. Under this transformation, Eq. (3.3) becomes

$$\begin{cases} \dfrac{d\varphi}{d\zeta} = (\varphi - c)y, \\ \dfrac{dy}{d\zeta} = g - c\varphi + \varphi + \dfrac{1}{2}\varphi^2 - y^2, \end{cases} \tag{3.5}$$

Eq. (3.3) and Eq. (3.5) have the same first integral as (3.4). Consequently, system (3.5) has the same topological phase portraits as system (3.3) except for the straight line $\varphi = c$. Obviously, $\varphi = c$ is an invariant straight-line solution for system (3.5).

Now we consider the singular points of system (3.5) and their properties. Note that for a fixed h, (3.4) determines a set of invariant curves of (3.5). As h is varied (3.4) determines different families of orbits of (3.5) having different dynamical behaviors. Let $M(\varphi_e, y_e)$ be the coefficient matrix of the linearized system of (3.5) at the equilibrium point (φ_e, y_e), then

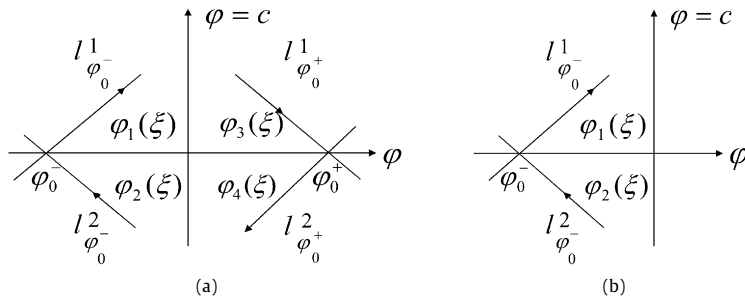$$M(\varphi_e, y_e) = \begin{pmatrix} y_e & \varphi_e - c \\ \varphi_e - (c - 1) & -2y_e \end{pmatrix}$$

Fig. 2. The sketches of orbits connecting with saddle points. (a) $g < g_2(c)$; (b) $g_2(c) \leqslant g \leqslant g_1(c)$.

and at this equilibrium point, we have

$$J(\varphi_e, y_e) = \det M(\varphi_e, y_e) = -2y_e^2 - (\varphi_e - c)[\varphi_e - (c - 1)],$$

$$p(\varphi_e, y_e) = \text{trace}(M(\varphi_e, y_e)) = -y_e^2 \leqslant 0.$$

By the theory of planar dynamical system (see [14]), for an equilibrium point of a planar dynamical system, if $J < 0$, then this equilibrium point is a saddle point; it is a center point if $J > 0$ and $p = 0$; if $J = 0$ and the Poincáre index of the equilibrium point is 0, then it is a cusp.

Since system (3.3) has the same topological phase portraits as system (3.5) except for the straight line $\varphi = c$. By investigating the topological dynamics of system (3.5), we can obtain the following properties for system (3.3).

(1) If $g < g_2(c)$, then system (3.4) has two equilibrium points $(\varphi_0^-, 0)$ and $(\varphi_0^+, 0)$. They are saddle points and there is inequality $\varphi_0^- < c - 1 < c < \varphi_0^+$. In this case, there are four orbits connecting with $(\varphi_0^-, 0)$, we use $l^1_{\varphi_0^-}$ and $l^2_{\varphi_0^-}$ to denote the two orbits lying on the right side of $(\varphi_0^-, 0)$ (see Fig. 2(a)). Meanwhile, there are four orbits connecting with $(\varphi_0^+, 0)$, we employ $l^1_{\varphi_0^+}$ and $l^2_{\varphi_0^+}$ to denote the two orbits lying on the left side of $(\varphi_0^+, 0)$ (see Fig. 2(a)).

(2) If $g_2(c) \leqslant g \leqslant g_1(c)$, then system (3.4) has two equilibrium points $(\varphi_0^-, 0)$, $(\varphi_0^+, 0)$. $(\varphi_0^-, 0)$ is a saddle point and $(\varphi_0^+, 0)$ is a center point or a degenerate center point. φ_0^- and φ_0^+ satisfy that $\varphi_0^- < c - 1 < \varphi_0^+ < c$. $l^1_{\varphi_0^-}$ and $l^2_{\varphi_0^-}$ are used to denote the two orbits lying on the right side of $(\varphi_0^-, 0)$ (see Fig. 2(b)).

(3) If $g_1(c) < g$, then system (3.4) has no equilibrium point.

On the $\varphi - y$ plane, the orbits $l^1_{\varphi_0^-}$, $l^2_{\varphi_0^-}$, $l^1_{\varphi_0^+}$ and $l^2_{\varphi_0^+}$ have the following expressions, respectively,

$$l^1_{\varphi_0^-}: \quad y = \frac{1}{2} \frac{(\varphi - \varphi_0^-)\sqrt{\varphi^2 + l_1\varphi + l_2}}{c - \varphi}, \tag{3.6}$$

$$l^2_{\varphi_0^-}: \quad y = \frac{1}{2} \frac{(\varphi_0^- - \varphi)\sqrt{\varphi^2 + l_1\varphi + l_2}}{c - \varphi}, \tag{3.7}$$

$$l^1_{\varphi_0^+}: \quad y = \frac{1}{2} \frac{(\varphi_0^+ - \varphi)\sqrt{\varphi^2 + m_1\varphi + m_2}}{\varphi - c}, \tag{3.8}$$

$$l^1_{\varphi_0^+}: \quad y = \frac{1}{2} \frac{(\varphi - \varphi_0^+)\sqrt{\varphi^2 + m_1\varphi + m_2}}{\varphi - c}, \tag{3.9}$$

where φ_0^- and φ_0^+ are in (2.2), l_1 and l_2 are in (2.9) and (2.10), m_1 and m_2 are in (2.12) and (2.13).

Assume that $\varphi = \varphi_1(\xi)$, $\varphi = \varphi_2(\xi)$, $\varphi = \varphi_3(\xi)$ and $\varphi = \varphi_4(\xi)$ on $l^1_{\varphi_0^-}$, $l^2_{\varphi_0^-}$, $l^1_{\varphi_0^+}$ and $l^2_{\varphi_0^+}$, respectively and $\varphi_1(0) = \varphi_2(0) = a$, $\varphi_3(0) = \varphi_4(0) = b$, where a and b are two constants, and $a \in (\varphi_0^-, c)$, $b \in (c, \varphi_0^+)$. Substituting (3.6)–(3.9) into the first equation of (3.3) and integrating along the corresponding orbits, respectively, we have

$$\int_a^{\varphi_1} \frac{c - s}{(s - \varphi_0^-)\sqrt{s^2 + l_1 s + l_2}} \, ds = \frac{1}{2} \int_0^\xi ds \quad (\text{along } l^1_{\varphi_0^-}), \tag{3.10}$$

$$\int_{\varphi_2}^a \frac{c - s}{(\varphi_0^- - s)\sqrt{s^2 + l_1 s + l_2}} \, ds = \frac{1}{2} \int_\xi^0 ds \quad (\text{along } l^2_{\varphi_0^-}), \tag{3.11}$$

$$\int_{\varphi_3}^b \frac{s - c}{(\varphi_0^+ - s)\sqrt{s^2 + m_1 s + m_2}} \, ds = \frac{1}{2} \int_\xi^0 ds \quad (\text{along } l^1_{\varphi_0^+}), \tag{3.12}$$
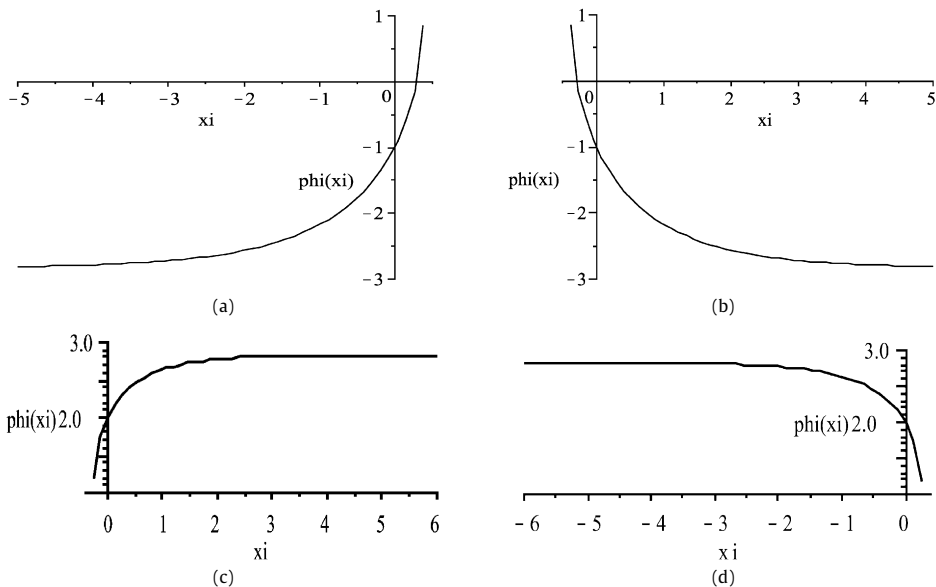
Fig. 3. The numerical simulations of integral curves of Eq. (3.2). (a) $\varphi(0) = -1$, $\varphi'(0) = 2.217532085$; (b) $\varphi(0) = -1$, $\varphi'(0) = -2.217532085$; (c) $\varphi(0) = 2$, $\varphi'(0) = 1.499467912$; (d) $\varphi(0) = 2$, $\varphi'(0) = -1.499467912$.

$$\int_b^{\varphi_4} \frac{s - c}{(s - \varphi_0^+)\sqrt{s^2 + m_1 s + m_2}} \, ds = \frac{1}{2} \int_0^{\xi} ds \quad \left(\text{along } l_{\varphi_0^+}^2\right). \tag{3.13}$$

Computing the above four integrals we obtain the implicit expressions of $\varphi_i(\xi)$ as (2.5)–(2.8).

Meanwhile, suppose that $\varphi_1(\xi) \to c$ as $\xi \to \xi_0^1$, $\varphi_2(\xi) \to c$ as $\xi \to -\xi_0^2$, $\varphi_3(\xi) \to c$ as $\xi \to -\xi_0^3$, $\varphi_4(\xi) \to c$ as $\xi \to \xi_0^4$, then it follow from (3.10)–(3.13) that

$$\xi_0^1 = \xi_0^2 = \int_a^c \frac{c - s}{(s - \varphi_0^-)\sqrt{s^2 + l_1 s + l_2}} \, ds \quad \left(\text{along } l_{\varphi_0^-}^1\right), \tag{3.14}$$

$$\xi_0^3 = \xi_0^4 = \int_b^c \frac{s - c}{(s - \varphi_0^+)\sqrt{s^2 + m_1 s + m_2}} \, ds \quad \left(\text{along } l_{\varphi_0^+}^2\right). \tag{3.15}$$

Computing the above two integrals, we get the expressions of ξ_0^1 and ξ_0^3 as in (2.25) and (2.26). The proof is finished.

4. Numerical simulations

In this section, we will simulate the planar graphs of the kink-like and the antikink-like waves.

From Section 3, we see that in the parameter expressions $\varphi = \varphi(\xi)$ and $y = y(\xi)$ of the orbits of system (3.3), the graph of $\varphi(\xi)$ and the integral curve of Eq. (3.2) are the same. In other words, the integral curves of Eq. (3.2) are the planar graphs of the traveling waves of Eq. (1.8). Therefore, we can see the planar graphs of the kink-like and the antikink-like waves through the simulation of the integral curves of Eq. (3.2).

Example 2. Take the same data as Example 1, that is $c = 1$, $g = -4$, $a = -1$, $b = 2$. Let $\varphi = a = -1$ in (3.6) and (3.7), then we can get $y \approx 2.217532085$ or $y \approx -2.217532085$. And let $\varphi = b = 2$ in (3.8) and (3.9), then we obtain $y \approx 1.499467912$ or $y \approx -1.499467912$. Thus we take the initial conditions of Eq. (3.2) as follows: (i) Corresponding to $l_{\varphi_0^-}^1$ we take $\varphi(0) = -1$ and $\varphi'(0) = 2.217532085$. (ii) Corresponding to $l_{\varphi_0^-}^2$ we take $\varphi(0) = -1$ and $\varphi'(0) = -2.217532085$. (iii) Corresponding to $l_{\varphi_0^+}^1$ we take $\varphi(0) = 2$ and $\varphi'(0) = 1.499467912$. (iv) Corresponding to $l_{\varphi_0^+}^2$ we take $\varphi(0) = 2$ and $\varphi'(0) = -1.499467912$.

Under each set of initial conditions we use Maple to simulate the integral curves of Eq. (3.2) as Fig. 3. Comparing Fig. 1 with Fig. 3, we can see that the graphs of $\varphi_i(\xi)$ ($i = 1, 2, 3, 4$) are the same as the simulation of integrals curve of Eq. (3.2). This implies that our theoretic results agree with the numerical simulations.

5. Conclusion

In this paper, we find new bounded waves for the Fornberg–Whitham equation (1.8). Their implicit expressions are obtained in (2.5)–(2.8). From the graphs (see Fig. 1) of the implicit functions and the numerical simulations (see Fig. 3) we see that these new bounded solutions are defined on some semifinal bounded domains and possess properties of kink waves and anti-kink waves.

Acknowledgments

References

[1] J. Lenells, Traveling wave solutions of the Camassa–Holm and Korteweg–de Vries equations, J. Nonlinear Math. Phys. 11 (2004) 508–520.
[2] B. Dey, Domain wall solutions of KdV like equations with higher order nonlinearity, J. Phys. A 19 (1986) L9–L12.
[3] J. Lenells, Traveling wave solutions of the Camassa–Holm equation, J. Differential Equations 217 (2005) 393–430.
[4] Z. Liu, C. Chen, Compactons in a general compressible hyperelastic rod, Chaos Solitons Fractals 22 (2004) 627–640.
[5] J. Lenells, Traveling wave solutions of the Degasperis–Procesi equation, J. Math. Anal. Appl. 306 (2005) 72–82.
[6] J. Nickel, Travelling wave solutions to the Kuramoto–Sivashinsky equation, Chaos Solitons Fractals 33 (2007) 1376–1382.
[7] Z. Liu, Q. Li, Q. Lin, New bounded traveling waves of Camassa–Holm equation, Internat. J. Bifur. Chaos 14 (2004) 3541–3556.
[8] B. Guo, Z. Liu, Two new types of bounded waves of CH-γ equation, Sci. China Ser. A 48 (2005) 1618–1630.
[9] M. Tang, W. Zhang, Four types of bounded wave solutions of CH-γ equation, Sci. China Ser. A 50 (2007) 132–152.
[10] C. Chen, M. Tang, A new type of bounded waves for Degasperis–Procesi equation, Chaos Solitons Fractals 27 (2006) 698–704.
[11] Z. Liu, L. Yao, Compacton-like wave and kink-like wave of GCH equation, Nonlinear Anal. Real World Appl. 8 (2007) 136–155.
[12] G.B. Whitham, Variational methods and applications to water wave, Proc. R. Soc. Lond. Ser. A 299 (1967) 6–25.
[13] B. Fornberg, G.B. Whitham, A numerical and theoretical study of certain nonlinear wave phenomena, Philos. Trans. R. Soc. Lond. Ser. A 289 (1978) 373–404.
[14] D. Luo, et al., Bifurcation Theory and Methods of Dynamical Systems, World Scientific Publishing Co., London, 1997.